J Water Environ Nanotechnol 2026, 11(3): 382-394
10.22090/jwent.2025.2074564.1979

RESEARCH PAPER

Synthesis and Characterization of *Parquetina Nigrescens* Plant-Mediated Zinc Oxide Nanoparticles and Evaluation of Their Antioxidant, Antifungal, and Antimicrobial Activity

***Friday Meshach Danjuma*[1,2*], *Mercy Oluwaseyi Bamigboye*[2], *Maryam Ahmed Fara*[1], *Joseph Ishaya Gudu*[2], *Samuel Aina Friday*[2]**

[1]Department of Science Laboratory Technology, Newland Polytechnic, Ilorin 240102, Kwara State, Nigeria
[2]Department of Industrial Chemistry, Faculty of Physical Science, University of Ilorin, Ilorin, Kwara State, Nigeria

*Corresponding Author(s)
Email:
friday.md@newlandpolytechnic.edu.ng

Article History:
Received: 2025-10-13
Revised: 2025-12-17
Accepted: 2025-12-24

How to cite this article
Danjuma FM, Bamigboye MO, Fara MA, Gudu JI, Friday SA. Synthesis and Characterization of Parquetina nigrescens Plant-Mediated Zinc Oxide Nanoparticles and Evaluation of Their Antioxidant, Antifungal, and Antimicrobial Activity. J Water Environ Nanotechnol 2026, 11(3): 382-394, DOI: 10.22090/jwent.2025.2074564.1979

HIGHLIGHTS

- ZnO nanoparticles were green-synthesized using Parquetina nigrescens leaf extract for the first time
- XRD confirmed a hexagonal wurtzite structure with average crystallite size of 15.6 nm
- ZnO NPs showed strong antioxidant, antibacterial, and antifungal

ABSTRACT

In the present work, zinc oxide nanoparticles (ZnO NPs) were biosynthesized using ethanolic leaf extract of *Parquetina nigrescens*, which acted as both reducing and stabilizing agents. The obtained nanoparticles were characterized using ultraviolet–visible (UV–Vis) spectroscopy, Fourier-transform infrared (FTIR) spectroscopy, X-ray diffraction (XRD), scanning electron microscopy (SEM), and thermogravimetric–differential thermal analysis (TGA–DTA). Phytochemical screening of the extract revealed the presence of alkaloids, flavonoids, saponins, tannins, and phenolic compounds. The UV–Vis spectrum showed a characteristic absorption peak at 414 nm, confirming nanoparticle formation, while FTIR analysis highlighted the involvement of phytochemicals in surface functionalization. XRD patterns confirmed a hexagonal wurtzite crystalline structure with an average crystallite size of 15.6 nm. SEM micrographs displayed porous, irregularly shaped, agglomerated nanoscale flakes. Thermal analysis indicated good stability, with sequential weight losses attributed to moisture evaporation and decomposition of residual organics. Antioxidant evaluation through the DPPH assay demonstrated strong radical scavenging activity (IC_{50} = 34.85 µg/mL). Antifungal tests revealed that ZnO NPs exhibited greater inhibitory effects than the crude extract, particularly against *Candida ethanolica* compared to *Saccharomyces cerevisiae*. Antibacterial assays showed pronounced activity against *Staphylococcus aureus* (ATCC 33863) and *Bacillus subtilis* (ATCC 23857), whereas *Salmonella typhi* (ATCC 19430) and *Pseudomonas aeruginosa* (ATCC 27853) were less susceptible. Collectively, these results indicate that *Parquetina nigrescens*-mediated ZnO NPs possess strong antioxidant, antibacterial, and antifungal properties, highlighting their promise as sustainable alternatives in biomedical and pharmaceutical applications.

KEYWORDS:

Green Synthesis; ZnO NPs; Characterization; Antioxidant; Antibacterial; Antifungal

©2026 The Author(s). Published by the Iranian Environmental Mutagen Society. This work is licensed under the Creative Commons Attribution 4.0 International License (CC BY 4.0). To view a copy of this license, visit http://creativecommons.org/licenses/by/4.0/.

INTRODUCTION

Nanotechnology is rapidly emerging as a cutting-edge technology with diverse applications in the chemical, pharmaceutical, mechanical, and food processing industries. It has also shown great potential in environmental sciences, drug delivery, computing, energy generation, and optics [1]. Since its inception, nanotechnology has enabled the creation of a wide range of nanoscale devices using chemical, physical, and biologically benign approaches. Among these efforts, green nanoparticle (NP) synthesis has piqued interest as a straightforward and adaptable technique [2].

Nanoparticles (NPs), defined as atomic-scale particles ranging from 1-100 nm, have distinct features due to their nanoscale dimensions and large surface area as compared to macroparticles [3]. Their size-related properties differ greatly from bulk materials [4], making them appropriate for a wide range of applications, including biosensors, nanomedicine, and bionanotechnology [3].

Conventional approaches to NP synthesis frequently have constraints such as lengthy processing periods, high costs, complex procedures, and reliance on harmful chemicals. These disadvantages have redirected the focus to eco-friendly and quick green synthesis techniques [5, 6]. Researchers have recently shifted their focus to more sustainable techniques of creating nanomaterials. In this context, plant-mediated green synthesis of NPs has emerged as a cost-effective, safe, and ecologically friendly option [7-9].

Green synthesised NPs are effective alternatives for chemically produced counterparts, reducing environmental toxicity [10, 11]. Importantly, plant-mediated nanoparticles frequently have better defined morphologies and particle sizes than those generated via physicochemical approaches [12]. Significant interest has been directed toward metal oxide nanoparticles (MO NPs) due to their distinct physical, chemical, and biological properties, such as solubility, stability, and adhesiveness [13].

Zinc oxide (ZnO) is one of the most promising inorganic oxides for nanoparticle biogenesis due to its distinct structural and functional characteristics. Its uses include medication delivery, solar cells, photocatalysis, and personal care goods such as sunscreens and cosmetics [14-19]. Zinc oxide nanoparticles (ZnO NPs) are useful because of their broad radiation absorption spectrum, high electrochemical coupling coefficient, and photostability [20]. As a result, ZnO NPs have been widely used in commercial items such as ceramics, cement, plastics, glass, ointments, lubricants, adhesives, sealants, pigments, batteries, ferrites, fire retardants, cosmetics, sunscreens, and nutritional supplements in food [21, 22].

Parquetina nigrescens, a perennial evergreen woody climber from the Apocynaceae family, was used in this study as a reducing and capping agent. *P. nigrescens* has long been utilized in African countries like Ghana, Nigeria, and Senegal to treat a variety of diseases [23]. Phytochemical studies have revealed alkaloids, cardenolides, and glycosides in the plant, which are responsible for its many biological activities [24]. Several investigations have confirmed its antioxidant, anti-inflammatory, antisickling, hematological, cytotoxic, antimicrobial, antipyretic, sympathomimetic, uterotonic, analgesic, and anti-ulcerogenic properties [25, 26].

Several plant species have already been used for plant extract-assisted synthesis of ZnO nanoparticles. For example, *Chrysophyllum albidum* fruit and leaf extracts were used to make ZnO NPs, which were then tested for antioxidant, anti-inflammatory, and antibacterial properties utilizing techniques such as XRD, SEM, EDX, TEM, UV-Vis, and FTIR [27]. The extract-mediated ZnO NPs demonstrated antioxidant activity, with EC50 values of 0.507 ± 0.015, 0.255 ± 0.006, 0.193 ± 0.003, and 0.004 ± 0.000 mg/mL for leaf, fruit, seed, and ascorbic acid, respectively. At 50 mg/mL, ZnO NPs derived from *C. albidum* seed extract had the maximum zone of inhibition (24.33 ± 0.47 mm) against *S. aureus* and the lowest (13.00 ± 1.41 mm) against *E. coli*, according to antibacterial tests. Fruit extract-mediated ZnO NPs showed the highest inhibition (18.00 ± 0.82 mm) against *C. albicans* at 50 mg/mL. The extract-mediated ZnO NPs had IC_{50} values for anti-inflammatory actions in the following order: fruit, seed, and leaf.

Similarly, ZnO NPs produced from *Pelargonium odoratissimum* aqueous leaf extract were characterized using UV-Vis, FTIR, XRD, DLS, HR-TEM, FE-SEM, and EDX, and their antioxidant, antibacterial, and anti-inflammatory activities were assessed [28]. XRD found an average crystallite size of 14 nm, but HR-TEM revealed hexagonal structures averaging 34.12 nm. FTIR analysis confirmed a ZnO stretching vibration at 436 cm^{-1}. Biosynthesized ZnO NPs demonstrated DPPH scavenging activity in antioxidant tests, with an IC50 of 28.11 μg/mL. Disk diffusion demonstrated high antibacterial action against Staphylococcus aureus (ATCC 8095), Pseudomonas aeruginosa (ATCC10662), and Escherichia coli (ATCC 25922), but Bacillus cereus (ATCC 13753) exhibited reduced sensitivity. Using the HRBC membrane stabilization method, anti-inflammatory activity was shown to be 95.6% at 1000 μg/mL, comparable to indomethacin.

In this study, *Parquetina nigrescens* leaf extract was used for the biogenic production of ZnO nanoparticles. UV-Vis spectroscopy, FTIR, XRD, TGA, and SEM were conducted to study the properties of the synthesized nanoparticles. Furthermore, their antioxidant and antibacterial properties were thoroughly studied against certain pathogenic strains. According to available literature, this is the first attempt at using *Parquetina nigrescens* leaf extract acting as a bio-reductant and surface-capping agent for the green synthesis of

ZnO nanoparticles, thus broadening the potential applications of this medicinal plant in nanobiotechnology.

MATERIALS AND METHODS

Chemicals

The materials used in this study included zinc acetate dihydrate ($Zn(CH_3COO)_2{\cdot}2H_2O$, ≥99%, Sigma-Aldrich, St. Louis, MO, USA), absolute ethanol (≥99.8%, Merck, Darmstadt, Germany), sodium hydroxide (NaOH, ≥98%, Sigma-Aldrich, St. Louis, MO, USA), phosphate buffer (pH 7.4, Sigma-Aldrich, St. Louis, MO, USA), sulfuric acid (H_2SO_4, 95-98%, Merck, Darmstadt, Germany), nitric acid (HNO_3, 65%, Merck, Darmstadt, Germany), chloroform ($CHCl_3$, ≥99%, Sigma-Aldrich, St. Louis, MO, USA), Wagner's solution (Sigma-Aldrich, St. Louis, MO, USA), ferric chloride ($FeCl_3$, ≥97%, Merck, Darmstadt, Germany), concentrated hydrochloric acid (HCl, 37%, Merck, Darmstadt, Germany), L-ascorbic acid (≥99%, Sigma-Aldrich, St. Louis, MO, USA), 2,2-diphenyl-1-picrylhydrazyl (DPPH, Sigma-Aldrich, St. Louis, MO, USA), and deionized distilled water.

Sample Collection and Preparation.

Fresh leaves of *Parquetina nigrescens* (Afzel.) Bullock were obtained in October 2024 from the botanical garden of the University of Ilorin in Ilorin, Kwara State, Nigeria. The plant material was authenticated at the University of Ilorin's Department of Plant Biology, and a voucher specimen (UILH/01/019/876) was deposited in the institutional herbarium for future reference. The leaves were thoroughly cleaned, beginning with tap water to eliminate pollutants and soil particles, followed by three rinses with distilled water. The cleaned leaves were air-dried in a well-ventilated facility at ambient temperature (25 ± 2°C) for 14 days, avoiding direct sunlight to preserve photosensitive phytochemicals. After complete desiccation, the material was pulverized with a sterile mortar and pestle to create a fine powder (particle size < 0.5 mm). Ethanolic extract was made by macerating 20 g of the leaf powder in 200 mL of pure ethanol (99.8%, Merck) in an amber glass bottle. The mixture was then incubated at 37°C for 24 hours in a temperature-controlled incubator with gentle shaking (100 rpm) to allow for maximum bioactive compound extraction. After incubation, the mixture was filtered through Whatman No. 1 filter paper (pore size 11 µm) to separate the solid residue and liquid extract. The clear green filtrate was collected and stored in sterile amber glass vials in a refrigerator at 4°C, protected from light, for up to 7 days before being used in nanoparticle synthesis and phytochemical analysis.

Phytochemical Test of Parquetina nigrescens Leaf Extract.

Qualitative phytochemical assays were performed to identify the presence of secondary metabolites including flavonoids, alkaloids, saponins, tannins, and phenolic compounds. Standard procedures were employed as described in previous studies [29-31].

Test for Flavonoids. (Alkaline Reagent Test): The extract (1 mL) was treated with 5 mL of NaOH. The presence of flavonoids was confirmed by the formation of an intense yellow color.

Test for Alkaloids (Wagner's Test): The solvent extract (1 mL) was acidified with 1 mL of 1.5% v/v HCl, and 1 mL of Wagner's reagent was added. The occurrence of alkaloids was indicated by the appearance of yellowish to brown precipitates.

Test for Saponins (Frothing Test): About 1 mL of the extract was diluted separately with 20 mL of distilled water and was shaken in a graduated cylinder for 15 min, after which a 1 cm foam layer was observed, which is indicative of saponins.

Test for Tannins and Phenolic Compounds (Ferric Chloride Test): the extract (1 mL) was treated with a few mL of 2-3 mL of 5% (w/v) neutral ferric chloride. The formation of a dark blue and/or bluish-black color product showed the presence of tannins and phenol.

Synthesis of Zinc Oxide Nanoparticles

Zinc oxide nanoparticles (ZnO NPs) were synthesized according to a previously established method [28, 32] with slight modifications. In brief, 6.0 g of zinc acetate dihydrate ($Zn(CH_3COO)_2{\cdot}2H_2O$; Sigma-Aldrich) was dissolved in 100 mL of the plant extract under continuous magnetic stirring at 60 °C for 2 hours. The resultant mixture was cooled to 25 °C and centrifuged (HERMLE Z326K) at 10,000 rpm for 10 minutes. The supernatant was discarded, and the pellet was subjected to three washing cycles with distilled water. The purified pellet was placed in a Petri plate and dried in an oven at 90 °C. The dried product was ground into a fine powder using a pestle and mortar and subsequently calcined at 500 °C for 2 hours to eliminate residual organic impurities. The final annealed ZnO NP powder was stored in an airtight glass vial for subsequent physical characterization and biological assays.

Characterization of Biosynthesized ZnO NPs.

The zinc oxide nanoparticles (ZnO NPs) synthesized from *Parquetina nigrescens* leaf extract were characterized using a suite of analytical techniques to determine their physicochemical properties [32]. The formation of ZnO NPs was initially confirmed by UV-Visible spectroscopy (PG Instruments T70), monitoring the reaction mixture within a 200–800 nm range. X-ray diffraction (XRD) analysis performed on a Rigaku MiniFlex 600 diffractometer identified the crystalline nature of the nanoparticles. The average size of crystallites was obtained usingScherrer's equation: $D = k\lambda / \beta\cos\theta$, where D is the crystallite size, k is the shape factor (0.94), λ is the X-ray wavelength (1.5421 Å), and β is the full width at half maximum (FWHM) at Bragg's angle θ. Fourier transform

J Water Environ Nanotechnol, 2026, 11(3): 382-394
10.22090/jwent.2025.2074564.1979

infrared (FTIR) spectroscopy (Shimadzu FTIR 8400 S, 400–4000 cm^{-1}) identified the functional groups involved in the synthesis and stabilization of the nanoparticles. The surface morphology and physical dimensions were examined by scanning electron microscopy (SEM; Phenom Prox model), while energy-dispersive X-ray spectroscopy (EDX) confirmed the elemental composition. Finally, thermal stability was assessed via thermogravimetric and differential thermal analysis (TG/DTA) using a TGA-Q500 series analyzer.

Antibacterial Assay

The antibacterial activity was evaluated against selected bacterial strains using the agar disc diffusion method (ADDM) [28, 33]. Briefly, sterile Whatman filter paper discs (6 mm diameter) were impregnated with 40 µL of different test solutions: three concentrations of ZnO NPs (15, 25, and 50 µg mL^{-1}) and *Parquetina nigrescens* leaf extract (25 µg mL^{-1}), all dissolved in ethanol. A solvent-only (ethanol) disc served as the negative control, while discs containing zinc acetate dihydrate and ciprofloxacin (5 µg) were used as additional and positive controls, respectively. Overnight bacterial cultures were adjusted to ~1 × 10^7 CFU mL^{-1} in LB broth and swabbed onto agar plates. Discs loaded with the samples were positioned on the agar plates, which were then incubated at 37 °C for 24 hrs. The antibacterial activity was quantified by measuring the zones of inhibition (ZOI) in millimeters. All assays were performed in duplicate.

Antifungal

The agar well diffusion method was used to assess antifungal activity [34, 35]. Assays were conducted on both Mueller-Hinton and potato dextrose agar plates. Wells were filled with ZnO NPs, *Parquetina nigrescens* leaf extract (15, 25, and 50 mg/mL), and 0.2 M zinc acetate, with ciprofloxacin and gentamicin used as positive controls. The inhibitory zones for these tests were assessed after 24 hours of incubation at 37°C. Separately, the antifungal efficacy of ZnO NPs and *Parquetina nigrescens* leaf extract was tested specifically against *Candida ethanolica* and *Saccharomyces cerevisiae* using potato dextrose agar plates. The same concentration range (15, 25, and 50 mg/mL) was used in each well. For this antifungal assay, inhibition zones were assessed after 48 hours of incubation at 28 °C.

Antioxidant Activities

The free radical scavenging activity of the *Parquetina nigrescens* leaf extract and the biosynthesized ZnO NPs was evaluated using the 2,2-diphenyl-1-picrylhydrazyl (DPPH) assay, following a described method [28, 34, 36]. Briefly, 0.1 mL of each sample or standard (L-ascorbic acid) at concentrations ranging from 5 to 100 µg mL^{-1} was mixed with 2 mL of a methanolic DPPH solution (25 mg L^{-1}). The reaction mixture was vortexed vigorously, incubated in the dark at 35 ± 2 °C for 30 minutes, after which the absorbance was measured at 517 nm using a UV-Vis spectrophotometer (Hitachi U-2900). All experiments were performed in triplicate. The free radical scavenging capacity (% inhibition) was calculated using the following formula:

$$\%\ \text{inhibition}\left(\%\ \text{Anti}-\text{radical activity}\right)=\frac{\text{A control}-\ \text{A sample}}{\text{A control}}\times 100 \quad (1)$$

in which A is taken as the absorbance

Statistical Analysis

All biological assays—including the antioxidant, antibacterial, and antifungal activity tests—were performed in triplicate, and the results are presented as mean ± standard deviation (SD). Statistical analysis was conducted using SPSS software (version 23, IBM Corporation, Armonk, NY, USA). A two-way analysis of variance (ANOVA) was employed, and differences were considered statistically significant at a p-value of less than 0.05.

RESULTS AND DISCUSSION

Phytochemical screening of Parquetina nigrescens

The ethanolic extract of *Parquetina nigrescens* leaves was subjected to phytochemical screening to identify the primary classes of secondary metabolites. Table 1 presents the qualitative tests carried out and the bioactive constituents detected. Understanding the correlation between phytochemicals and the biological activities of medicinal plants is fundamental, as these metabolites often serve as precursors for the development of therapeutic agents with targeted functions. The extract was obtained through ethanol-based decoction, yielding a concentrated green residue. The analysis confirmed the presence of several key phytoconstituents, consistent with earlier reports on this species [29–31].

Characterization of ZnO NPs

UV-Vis Spectroscopy

The optical characteristics of the biosynthesized ZnO nanoparticles mediated by *Parquetina nigrescens* leaf extract were examined using UV–Visible spectrophotometry. As shown in Fig. 1, the absorption spectrum exhibited a distinct peak at 414 nm, which is indicative of ZnO nanoparticle formation. This absorption feature arises from surface plasmon resonance (SPR) effects coupled with organic–metal interactions between phytochemicals and zinc ions [37, 38]. Similar spectral behavior has been reported in earlier studies, such as the work of [35], where *Verbascum sinaiticum* extract was employed in ZnO nanoparticle synthesis. Variations in the absorption maxima observed across studies are often attributed

Table 1. Qualitative phytochemical screening of *Parquetina nigrescens* leaf extracts

S/N	Phytochemical	Detection Test	Results
1	Alkaloids	Wagner	+
2	Tannins	Ferric Chloride	+
3	Saponins	Frothing	+
4	Phenolics	Ferric Chloride	+
5	Flavonoids	Alkaline	+

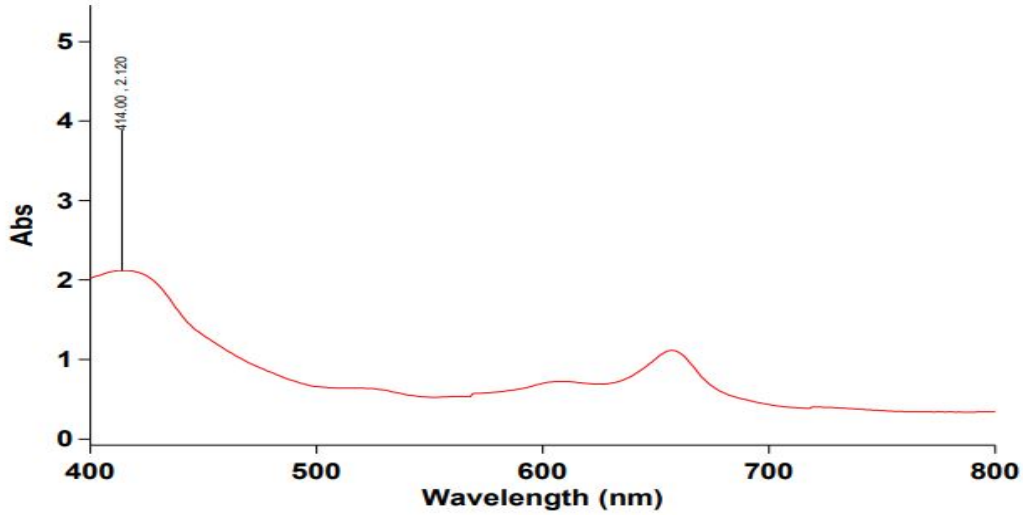

Fig. 1. Absorption spectrum of *Parquetina nigrescens* synthesized ZnO NPs

to differences in synthesis parameters, including temperature, extract concentration, pH, reaction duration, and precursor ion availability [39-43].

The optical bandgap energy (Eg) was determined using the equation:

$$EG = HC/\lambda \quad (2)$$

where h represents Planck's constant (6.626×10^{-34} J·s), c is the speed of light (3×10^{8} m/s), and λ is the absorption wavelength (414 nm). The calculated bandgap was 3.00 eV. This value, lower than the intrinsic bandgap of bulk ZnO (~3.37 eV), suggests a red-shifted absorption edge. Rather than being governed by quantum confinement, this shift is more plausibly associated with defect-related sub-bandgap states, such as oxygen vacancies, generated during green synthesis. The pronounced UV absorption capacity of these ZnO nanoparticles underscores their potential in biomedical and industrial applications, including sunscreen formulations and antibacterial agents [14, 28].

FTIR

FTIR spectroscopy was employed to elucidate the functional groups present in the *Parquetina nigrescens* leaf extract and their involvement in the reduction and stabilization of ZnO nanoparticles. The spectra of the synthesized ZnO NPs are presented in Fig. 2 and Table 2. A moderate absorption band observed at 3645 cm^{-1}, along with a peak at 3084 cm^{-1}, corresponds to O–H stretching vibrations, characteristic of alcohols, phenolics, and flavonoid compounds [44, 45]. A low-intensity signal at 2967 cm^{-1} is assigned to C–H stretching modes typically associated with hydroxyl-containing compounds [46, 47]. The absorption at 1558 cm^{-1} represents C=C stretching vibrations from aromatic rings [48, 49], while the strong peaks at 1056 and 1017 cm^{-1} are attributed to C–O stretching vibrations of aromatic alcohols and phenolic groups (Table 1). For the nanoparticle spectra, distinct absorption features appeared in the low wavenumber region, with bands recorded at 635 cm^{-1} [35], 682 cm^{-1} [50], and 682 cm^{-1} [51], closely matching the characteristic Zn–O stretching vibration. In the present study, the ZnO nanoparticles displayed a sharp band at 689 cm^{-1}, further confirming their successful formation. Overall, FTIR analysis demonstrates that phytoconstituents such as flavonoids and phenols are actively involved as reducing, stabilizing, and capping agents during the green synthesis of ZnO nanoparticles [52].

J Water Environ Nanotechnol, 2026, 11(3): 382-394
10.22090/jwent.2025.2074564.1979

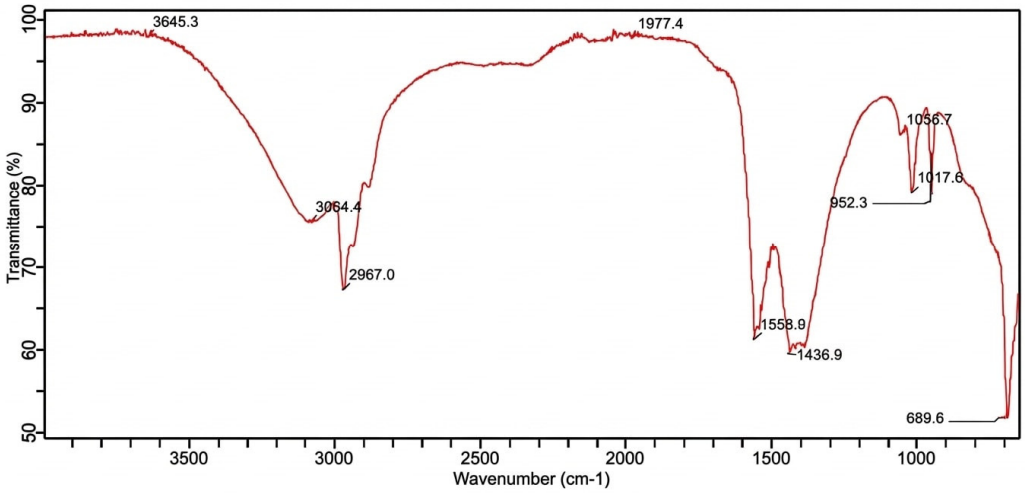

Fig. 2. FTIR spectrum of *Parquetina nigrescens* synthesized ZnO NPs

Table 2. FTIR peak assignments for *Parquetina nigrescens* leaf extract and ZnO nanoparticles

Wavenumber (cm^{-1})	Assignment	Functional Group/Compound
3645–3084 (broad)	O–H stretching	Phenols, flavonoids, alcohols, water
2967	C–H stretching	Aliphatic CH_2 and CH_3 groups
1558	C=C stretching	Surface-bound aromatics
1056, 1017	C–O stretching	Alcohols, phenols, ethers, glycosides
1438	COO^-	carboxylates
952	C–H out-of-plane bending	glycosidic linkages
689	Zn–O stretching	Zinc oxide lattice vibration

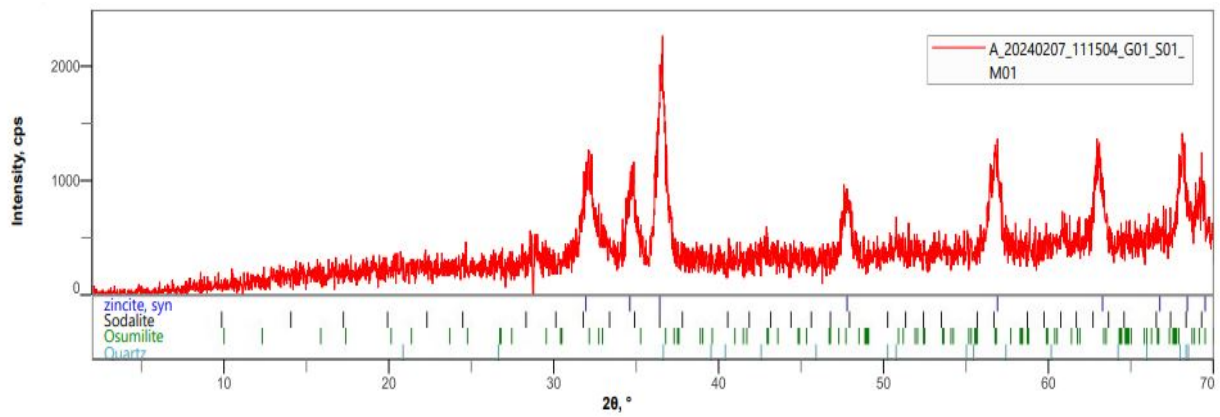

Fig. 3. XRD pattern of *Parquetina nigrescens*-synthesized ZnO NPs

XRD analysis

The structural crystallinity and phase composition of ZnO nanoparticles synthesized using *Parquetina nigrescens* extract were examined by XRD (Fig. 3). The diffraction pattern displayed prominent peaks at 2θ values of 32.13°, 34.74°, 36.53°, 47.76°, 56.81°, and 67.99°, which correspond to the (110), (101), (111), (002), (211), (103), and (410) lattice planes, respectively. These reflections match well with the standard Joint Committee on Powder Diffraction Standards (JCPDS card No. 04-013-6608), confirming the hexagonal wurtzite

structure of ZnO [53]. The absence of secondary peaks indicates that the biosynthesized nanoparticles are phase-pure [37].

The crystallite size (D) was estimated using the Debye–Scherrer equation:

$$D=KD = K\lambda / \beta \cos \theta \quad (3)$$

where K is the shape factor (0.94), λ is the X-ray wavelength (1.5406 Å), β is the full width at half maximum (FWHM) of the diffraction peak in radians, and θ is the Bragg angle. Based on the most intense (101) reflection at 36.50°, the mean crystallite size was calculated to be approximately 15.6 nm.

The relatively small crystallite size and large surface-to-volume ratio are advantageous for biological applications, as they enhance interactions with microbial membranes, promote reactive oxygen species (ROS) generation, and contribute to antimicrobial activity [37, 38]. The narrow, intense diffraction peaks further indicate high crystallinity, while the absence of additional reflections confirms the structural stability and phase purity of the ZnO nanoparticles [54, 55].

SEM

The surface morphology of the biosynthesized ZnO nanoparticles was examined by SEM, as illustrated in Fig. 4. The micrograph revealed granular nanoparticles distributed across irregular, porous flake-like structures. Most particles appeared below 100 nm in diameter; however, evidence of aggregation into larger clusters was observed. Such agglomeration is commonly attributed to high surface energy, electrostatic attraction, and strong van der Waals interactions between adjacent nanoparticles [56]. The obtained morphology is consistent with reports from other green synthesis studies. For instance, ZnO nanoparticles prepared using *Euphorbia petiolata* extract exhibited aggregated, sponge-like structures [57], while those synthesized from *Calotropis gigantea* extract showed irregular spherical particles with pronounced clustering [58]. These comparisons highlight that nanoparticle agglomeration is a common phenomenon in phytomediated synthesis, largely influenced by plant extract composition and synthesis conditions.

Thermogravimetry/Differential Thermal Analysis (TG/DTA)

The thermal stability and compositional features of the biosynthesized ZnO nanoparticles were investigated using TGA/DTA (Fig. 5). The analysis was carried out in a nitrogen atmosphere at a heating rate of 10 °C/min over a temperature range of 30–900 °C. The overall weight loss occurred in multiple stages, leaving a final residue of 19.6% at 900 °C. The initial mass reduction of approximately 4% between 50 and 220 °C can be attributed to the release of adsorbed moisture and volatile surface-bound species. A subsequent weight loss of 14.19% occurred around 262.4 °C, corresponding to the thermal degradation of residual phytochemical moieties from the *Parquetina nigrescens* extract, which served as stabilizing and reducing agents during nanoparticle synthesis [59]. A

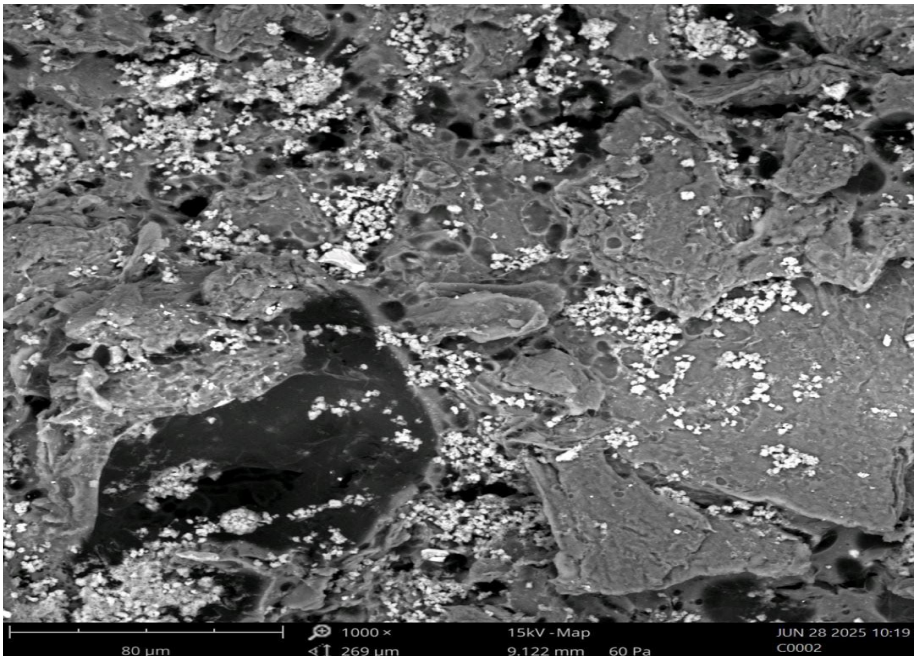

Fig. 4. SEM micrograph of *Parquetina nigrescens*-synthesized ZnO NPs

J Water Environ Nanotechnol, 2026, 11(3): 382-394
10.22090/jwent.2025.2074564.1979

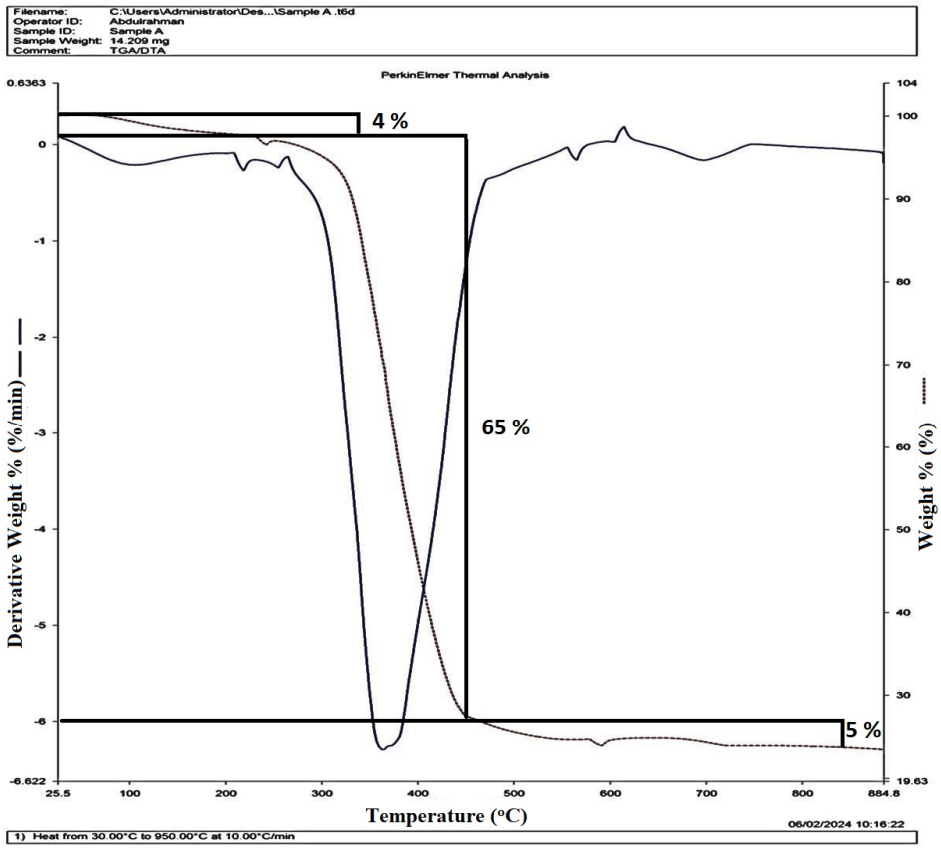

Fig. 5. TG/DTA spectra of *Parquetina nigrescens* synthesized ZnO NPs

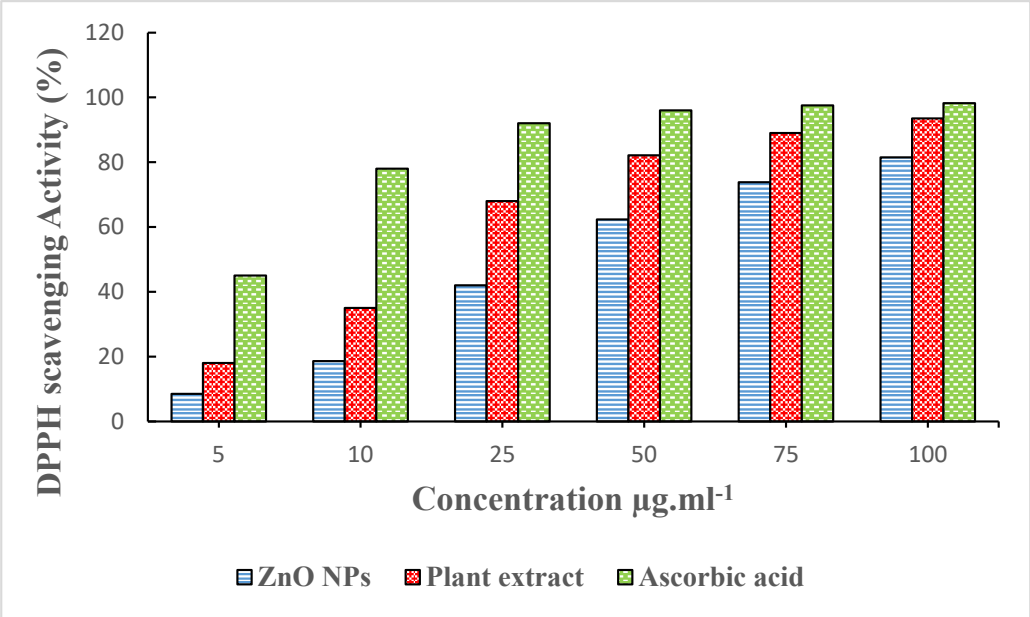

Fig. 6. DPPH radical scavenging activity of ZnO NPs, *Parquetina nigrescens* leaf extract, and L-ascorbic acid at different concentrations (5–100 µg/mL). Data points represent mean ± standard deviation (SD) from three independent experiments (n=3). IC_{50} values: ZnO NPs = 34.85 ± 0.03 µg/mL; *P. nigrescens* extract = 16.82 ± 0.01 µg/mL; L-ascorbic acid = 5.76 ± 0.02 µg/mL

major decomposition event was observed at 473 °C, accounting for 61.23% mass loss, after which no further significant changes were detected up to 800 °C [60]. The DTG profile (blue curve) revealed distinct peaks at approximately 300 and 450 °C, marking the maximum degradation rates. These transitions confirm the decomposition of organic constituents followed by the stabilization of the crystalline ZnO phase. Collectively, the TGA/DTA results demonstrate that the synthesized ZnO nanoparticles exhibit excellent thermal stability beyond 500 °C, making them suitable for applications requiring high-temperature tolerance.

DPPH

The antioxidant potential of ZnO nanoparticles, the ethanolic leaf extract of *Parquetina nigrescens*, and L-ascorbic acid was evaluated using the DPPH radical scavenging assay (Fig. 6). In all cases, radical scavenging activity increased in a concentration-dependent manner within the tested range of 5–100 μg mL^{-1}. At the highest concentration, the ZnO NPs achieved 81.5% inhibition, the plant extract reached 93.5%, while the ascorbic acid standard exhibited 98.2% inhibition. Dose–response analysis revealed half-maximal inhibitory concentration (IC_{50}) values of 34.85 μg mL^{-1} for ZnO NPs, 16.82 μg mL^{-1} for the *P. nigrescens* extract, and 5.76 μg mL^{-1} for L-ascorbic acid. These findings indicate that the plant extract exhibits considerably stronger antioxidant activity than the nanoparticles and a level of efficacy comparable to other medicinal plants, such as *Pelargonium graveolens* (IC_{50} = 16.59 μg mL^{-1}) [61]. The pronounced activity of the *P. nigrescens* extract is attributed to its high content of phenolic and flavonoid compounds, which are widely recognized for their ability to donate hydrogen atoms and neutralize free radicals [62]. These phytochemicals also serve as efficient bioreductants, participating in nanoparticle nucleation, capping, and stabilization through their hydroxyl (-OH) functional groups [62, 63]. Consistent with this role, *P. nigrescens* was found to possess substantial total phenolic (24.62 mg GAE/g) and flavonoid (16.01 mg RE/g) contents Table 3. Collectively, these results demonstrate that the phytoconstituents of *Parquetina nigrescens* not only impart significant antioxidant activity but also facilitate the eco-friendly synthesis and stability of ZnO nanoparticles.

Values are expressed as mean ± standard deviation of triplicates. Different superscript letters (a, b, c) within the same column indicate statistically significant differences ($p < 0.05$). DW = dry weight; GAE = gallic acid equivalents; RE = rutin equivalents; – = not determined.

Antibacterial

The antibacterial efficacy of the biosynthesized ZnO nanoparticles (NPs) was assessed against two Gram-positive bacteria, *Staphylococcus aureus* (ATCC 33863) and *Bacillus subtilis* (ATCC 23857) and two Gram-negative bacteria *Salmonella typhi* (ATCC 19430) and *Pseudomonas aeruginosa* (ATCC 27853) using the disc diffusion method. As summarized in Table 4, the ZnO NPs derived from *Parquetina nigrescens* extract demonstrated significant antibacterial activity against all tested pathogens. The highest susceptibility was observed in *B. subtilis*, with an inhibition zone of 24 ± 1.1 mm, followed by *S. aureus* (22 ± 0.50 mm), *S. typhi* (18 ± 1.0 mm), and *P. aeruginosa* (16 ± 0.90 mm). In

Table 3. IC_{50}, total phenolic content (TPC), and total flavonoid content (TFC) of *Parquetina nigrescens* leaf extract

Treatment	DPPH IC_{50} (μg mL–1)	TPC (mg GAE/g Dry plant extract)	TFC (mg GAE/g Dry plant extract)
Plant extract	16.82 ± 0.01^{b}	24.62 ± 0.31	16.01 ± 0.02
ZnO NPs	34.85 ± 0.03^{a}	-	-
L-Ascorbic acid	5.76 ± 0.02^{c}	-	-

Table 4. Antibacterial activity of ZnO NPs at different concentrations

Pathogenic Bacteria	Diameter of Inhibition Zone (mm)			Positive control Ciprofloxacin (5 μg disk)	Plant Extract (25 μg mL^{-1})
	ZnO NPs				
	15 μg mL^{-1}	25 μg mL^{-1}	50 μg mL^{-1}		
S. aureus	12 ± 0.6^{a}	16 ± 0.7^{b}	22 ± 0.5^{f}	28 ± 0.6^{c}	10 ± 0.3^{e}
P. aeruginosa	9.0 ± 0.4^{c}	12 ± 0.7^{e}	16 ± 0.9^{b}	23 ± 0.7^{a}	7 ± 0.2^{d}
S. typhi	10 ± 0.5^{d}	14 ± 0.6^{f}	18 ± 1.0^{a}	25 ± 0.2^{e}	8 ± 0.7^{g}
B. subtilis	13 ± 0.5^{f}	18 ± 0.1^{b}	24 ± 1.1^{c}	30 ± 3.1^{a}	11 ± 0.3^{d}

Values are means (n = 3). The superscript lettered (a-f) indicate significant differences (at $p < 0.05$) when subjected to SPSS test. The findings are given as mean ± standard deviation

J Water Environ Nanotechnol, 2026, 11(3): 382-394
10.22090/jwent.2025.2074564.1979

Table 5. Antifungal activity of ZnO NPs at different concentrations

Fungi	Diameter of Inhibition Zone (mm)			Gentamicin (20 µg/mL disk)	DMSO	Plant Extract (25 µg mL^{-1})
	ZnO NPs					
	15 µg mL^{-1}	25 µg mL^{-1}	50 µg mL^{-1}			
C. ethanolica	12.8 ± 0.4^{a}	17.5 ± 0.6^{c}	22.3 ± 0.5^{b}	25.1 ± 0.8^{a}	n.i	13.6 ± 0.1^{a}
S. cerevisiae	11.4 ± 0.3^{b}	15.2 ± 0.5^{a}	20.1 ± 0.6^{a}	23.8 ± 0.7^{d}	n.i	11.2 ± 0.0^{c}

n.i = no inhibition. Values are means (n = 3). The findings are given as mean ± standard deviation (at $p < 0.05$) when subjected to the SPSS test.

contrast, the *P. nigrescens* extract alone showed only moderate activity, with zones ranging from 7 ± 0.23 to 11 ± 0.25 mm. Notably, the biosynthesized ZnO NPs exhibited superior antibacterial performance compared to both the plant extract and the standard antibiotic ciprofloxacin. A clear differential susceptibility was noted, with Gram-positive bacteria being more effectively inhibited than Gram-negative strains. This trend is consistent with established literature, which attributes the variation to fundamental differences in cell wall structure [64, 65]. The thick, porous peptidoglycan layer of Gram-positive bacteria may facilitate the adhesion and accumulation of ZnO NPs and enhance electrostatic interactions with Zn^{2+} ions [66]. Conversely, the complex outer membrane of Gram-negative bacteria, rich in lipopolysaccharides, provides an additional permeability barrier that limits nanoparticle penetration and contributes to higher innate resistance [67–69]. Such structural resilience in Gram-negative bacteria is a recognized factor in the emergence of multidrug-resistant infections [70–73]. These findings align with previous studies. For instance, ZnO NPs synthesized using *Laurus nobilis* leaf extract were reported to be more effective against *S. aureus* (Gram-positive) than *P. aeruginosa* (Gram-negative), a phenomenon similarly explained by the differential cell wall architectures that govern nanoparticle interaction [28, 74, 75]. Furthermore, a dose-dependent increase in antibacterial activity was observed, where higher concentrations of ZnO NPs resulted in larger zones of inhibition. This is likely due to enhanced diffusion of a greater number of nanoparticles within the agar medium, as previously documented [76]. The antibacterial mechanism of ZnO NPs is multifactorial. Primarily, they exert toxicity through the release of Zn^{2+} ions, which disrupt critical enzymatic activities and metabolic pathways [77, 78]. Secondly, the generation of reactive oxygen species (ROS) by ZnO NPs induces oxidative stress, causing damage to cellular components such as proteins, lipids, and DNA [79, 80]. Finally, direct physical interaction and attachment of the nanoparticles to the bacterial cell surface can lead to membrane disruption, loss of integrity, and leakage of intracellular contents, culminating in cell death [81].

Antifungal

The antifungal activity of biosynthesized ZnO nanoparticles (ZnO NPs) and *Parquetina nigrescens* extract was evaluated against *Candida ethanolica* and *Saccharomyces cerevisiae* at concentrations of 15, 25, and 50 mg/mL as summarized in Table 5. The agar diffusion method was employed, and inhibition zones were measured in triplicate using a ruler (mm) [35]. Across all tested concentrations, ZnO NPs demonstrated significantly larger inhibition zones compared to *P. nigrescens*, with both treatments exhibiting a clear dose-dependent increase in antifungal activity [81]. Gentamicin (20 µg/mL) served as the positive control and produced substantial inhibition zones of 25.1 ± 0.80 mm against *C. ethanolica* and 23.8 ± 0.70 mm against *S. cerevisiae*, whereas the negative control (DMSO) showed no activity (0.00 ± 0.00 mm). Notably, ZnO NPs displayed stronger antifungal activity than the plant extract, with maximum inhibition observed at 50 mg/mL, particularly against *C. ethanolica*. This trend is in agreement with previous studies reporting the superior fungicidal activity of green-synthesized ZnO NPs over crude plant extracts [35, 82]. The enhanced antifungal efficacy of ZnO NPs may be attributed to their nanoscale dimensions, which confer a high surface-to-volume ratio, facilitating stronger adhesion and interaction with fungal cell surfaces. These interactions can induce structural membrane damage, disrupt cell permeability, and trigger the generation of reactive oxygen species (ROS), leading to oxidative stress and cell death. Such mechanisms explain the greater inhibitory effects of ZnO NPs compared to *P. nigrescens* extract [38, 83].

CONCLUSION

This study successfully demonstrates the usefulness of *Parquetina nigrescens* leaf extract as a new, green, and sustainable reducing and capping agent for the manufacture of zinc oxide nanoparticles. Comprehensive analysis revealed the synthesis of ZnO NPs with a crystalline, hexagonal wurtzite structure and an average size of 15.6 nm. The biosynthesized ZnO NPs outperformed the crude plant extract in terms of biological activity. They showed considerable dose-dependent antibacterial efficiency, particularly against Gram-positive bacteria, as well as robust antifungal activity. Furthermore, the nanoparticles demonstrated significant free radical scavenging activity in the DPPH assay, validating their antioxidant properties. The improved bioactivity is due to the synergistic effect of ZnO's nanoscale features, such as its high

surface area-to-volume ratio, and the phytochemicals from *P. nigrescens* that coat the nanoparticles. These findings not only highlight a traditional medicinal herb but also provide a simple, environmentally friendly method for producing ZnO NPs. The resulting nanoparticles hold great promise for use in biomedical therapeutics, particularly as active ingredients in topical antimicrobial formulations, wound healing agents, and antioxidant-based therapies, highlighting green nanotechnology's potential to contribute to advanced healthcare solutions.

Conflict of Interest
The authors declare no conflict of interest.

Funding
This study was not supported by any funding.

Author's Contributions
Study Conception or Design: Friday Meshach Danjuma, Mercy Oluwaseyi Bamigboye
Data Acquisition: Friday Meshach Danjuma, Maryam Ahmed Fara, Joseph Ishaya Gudu
Data Analysis or Interpretation: Friday Meshach Danjuma, Samuel Aina Friday
Manuscript Drafting: Friday Meshach Danjuma
Critical Manuscript Revision: Friday Meshach Danjuma, Mercy Oluwaseyi Bamigboye, Samuel Aina Friday
All authors have approved the final manuscript and are responsible for all aspects of the work.

AI Statement
The authors confirm that no AI tools or services were used during the preparation of this work.

Availability of data and materials
The datasets generated and/or analyzed during the current study are available from the corresponding author on reasonable request.

REFERENCES

1. Ramsden, J., 2016. *Nanotechnology: An Introduction*. William Andrew.
2. Albrecht, M.A., C.W. Evans and C.L. Raston, 2006. Green chemistry and the health implications of nanoparticles. *Green Chem.*, 8(5): 417–423. https://doi.org/10.1039/b517131h
3. Ashe, B., 2011. A detailed investigation to observe the effect of zinc oxide and silver nanoparticles in biological systems. MSc thesis, National Institute of Technology Rourkela. http://ethesis.nitrkl.ac.in/2741/
4. Buzea, C., I.I. Pacheco and K. Robbie, 2007. Nanomaterials and nanoparticles: Sources and toxicity. *Biointerphases*, 2(4): MR17–MR71. https://doi.org/10.1116/1.2815690
5. Herlekar, M., S. Barve and R. Kumar, 2014. Plant-mediated green synthesis of iron nanoparticles. *J. Nanopart.*, 2014: 1–9. https://doi.org/10.1155/2014/140614
6. Simonis, F. and S. Schilthuizen, 2006. *Nanotechnology: Innovation Opportunities for Tomorrow's Defence*. TNO Science and Industry Future Technology Center.
7. Iravani, S., 2011. Green synthesis of metal nanoparticles using plants. *Green Chem.*, 13(10): 2638–2650. https://doi.org/10.1039/c1gc15386b
8. Duan, H., D. Wang and Y. Li, 2015. Green chemistry for nanoparticle synthesis. *Chem. Soc. Rev.*, 44(16): 5778–5792. https://doi.org/10.1039/c4cs00363b
9. Bala, N., S. Saha, M. Chakraborty, M. Maiti, S. Das, R. Basu and P. Nandy, 2015. Green synthesis of zinc oxide nanoparticles using *Hibiscus subdariffa* leaf extract: Effect of temperature on synthesis, antibacterial and antidiabetic activity. *RSC Adv.*, 5(1): 4993–5003.
10. Mahanty, A., S. Mishra, R. Bosu, U. Maurya, S.P. Netam and B. Sarkar, 2013. Phytoextract-synthesized silver nanoparticles inhibit bacterial fish pathogen *Aeromonas hydrophila*. *Indian J. Microbiol.*, 53(4): 438–446. https://doi.org/10.1007/s12088-013-0409-9
11. Rafique, M., I. Sadaf, M.S. Rafique and M.B. Tahir, 2016. A review on green synthesis of silver nanoparticles and their applications. *Artif. Cells Nanomed. Biotechnol.*, 45(7): 1272–1291. https://doi.org/10.1080/21691401.2016.1241792
12. Raveendran, P., J. Fu and S.L. Wallen, 2003. Completely green synthesis and stabilization of metal nanoparticles. *J. Am. Chem. Soc.*, 125(46): 13940–13941. https://doi.org/10.1021/ja029267j
13. Ahmad, W. and D. Kalra, 2020. Green synthesis, characterization and antimicrobial activities of ZnO nanoparticles using *Euphorbia hirta* leaf extract. *J. King Saud Univ. Sci.*, 32(4): 2358–2364. https://doi.org/10.1016/j.jksus.2020.03.014
14. Agarwal, S., L.K. Jangir, K.S. Rathore, M. Kumar and K. Awasthi, 2019. Morphology-dependent structural and optical properties of ZnO nanostructures. *Appl. Phys. A*, 125(8). https://doi.org/10.1007/s00339-019-2852-x
15. Muthuvel, A., M. Jothibas and C. Manoharan, 2020. Effect of chemical synthesis compared to biosynthesized ZnO nanoparticles using *Solanum nigrum* leaf extract and their photocatalytic, antibacterial and in vitro antioxidant activity. *J. Environ. Chem. Eng.*, 8(2): 103705. https://doi.org/10.1016/j.jece.2020.103705
16. Bala, N., S. Saha, M. Chakraborty, M. Maiti, S. Das, R. Basu and P. Nandy, 2014. Green synthesis of zinc oxide nanoparticles using *Hibiscus subdariffa* leaf extract: Effect of temperature on synthesis, antibacterial and antidiabetic activity. *RSC Adv.*, 5(7): 4993–5003. https://doi.org/10.1039/c4ra12784f
17. Yusof, H.M., R. Mohamad, U.H. Zaidan and N.A.A. Rahman, 2019. Microbial synthesis of zinc oxide nanoparticles and their potential application as an antimicrobial agent and feed supplement. *J. Anim. Sci. Biotechnol.*, 10(1). https://doi.org/10.1186/s40104-019-0368-z
18. Bandeira, M., M. Giovanela, M. Roesch-Ely, D.M. Devine and J. da Silva Crespo, 2020. Green synthesis of zinc oxide nanoparticles: A review of synthesis methodology and mechanism. *Sustain. Chem. Pharm.*, 15: 100223. https://doi.org/10.1016/j.scp.2020.100223
19. Davar, F., A. Majedi and A. Mirzaei, 2015. Green synthesis of ZnO nanoparticles and application in dye degradation. *J. Am. Ceram. Soc.*, 98(6): 1739–1746. https://doi.org/10.1111/jace.13467
20. Kołodziejczak-Radzimska, A. and T. Jesionowski, 2014. Zinc oxide—from synthesis to application: A review. *Materials*, 7(4): 2833–2881. https://doi.org/10.3390/ma7042833
21. Sirelkhatim, A., S. Mahmud, A. Seeni, N.H.M. Kaus, L.C. Ann, S.K.M. Bakhori, H. Hasan and D. Mohamad, 2015. Review on zinc oxide nanoparticles: Antibacterial activity and toxicity mechanism. *Nano-Micro Lett.*, 7(3): 219–242. https://doi.org/10.1007/s40820-015-0040-x

22. Eixenberger, J.E., C.B. Anders, R.J. Hermann, R.J. Brown, K.M. Reddy, A. Punnoose and D.G. Wingett, 2017. Rapid dissolution of ZnO nanoparticles induced by biological buffers impacts cytotoxicity. *Chem. Res. Toxicol.*, 30(8): 1641–1651. https://doi.org/10.1021/acs.chemrestox.7b00136
23. Ayoola, A., O. Akinloye, O.O. Oguntibeju, J. Oke and A. Odetola, 2011. Antioxidant activities of *Parquetina nigrescens*. *Afr. J. Biotechnol.*, 10(24): 4920–4925.
24. Marks, W., H. Fong, T.W. Ma and N. Farnsworth, 1975. Cytotoxic principles of *Parquetina nigrescens*. *J. Pharm. Sci.*, 64(10): 1674–1676. https://doi.org/10.1002/jps.2600641019
25. Adase, E., P. Ankutse, D. Kumadoh, M. Archer, M.O. Kyene, G.N. Yeboah and D.O.A. Agyare, 2022. A review of *Parquetina nigrescens*: Phytochemical and pharmacological properties. *Evid.-Based Complement. Altern. Med.*, 2022: 1–21. https://doi.org/10.1155/2022/6076707
26. O.A.I., 2014. In vivo antityphoid activities and proximate analysis of ethanolic leaf extracts of *Parquetina nigrescens*. *IOSR J. Pharm. Biol. Sci.*, 9(5): 115–123. https://doi.org/10.9790/3008-0955115123
27. Droepenu, E.K., N.A.N. Jackson, M.O. Kyene, F. Ayertey, H. Brew-Daniels, T. Mensah, C. Adomako, A.P. Nartey, A.O. Gyampoh and L.A. Boamah, 2022. Plant-mediated ZnO nanostructures and biological activity. *J. Nanomater.*, 2022(1). https://doi.org/10.1155/2022/5508224
28. Abdelbaky, A.S., T.A. Abd El-Mageed, A.O. Babalghith, S. Selim and A.M.H.A. Mohamed, 2022. Green synthesis of ZnO nanoparticles using *Pelargonium odoratissimum*. *Antioxidants*, 11: 1444. https://doi.org/10.3390/antiox11081444
29. Gebreslassie, H. and A. Eyasu, 2019. Phytochemical screening of *Calpurnia aurea* leaf extract. *Int. J. Clin. Chem. Lab. Med.*, 5(4). https://doi.org/10.20431/2455-7153.0504004
30. Ganesan, K., S. Kumar, P. Nair, N. Letha and G. Banu, 2016. Phytochemical screening of *Phytolacca dodecandra* extracts.
31. Firisa, S.G., G.G. Muleta and A.A. Yimer, 2022. Synthesis of NiO and Cu-doped NiO nanocomposites using *Phytolacca dodecandra*. *ACS Omega*, 7(49): 44720–44732. https://doi.org/10.1021/acsomega.2c04042
32. Faisal, S., H. Jan, S.A. Shah, S. Shah, A. Khan, M.T. Akbar, M. Rizwan, F. Jan, N. Wajidullah, N. Akhtar, A. Khattak and S. Syed, 2021. Green synthesis of ZnO nanoparticles using *Myristica fragrans*. *ACS Omega*, 6(14): 9709–9722. https://doi.org/10.1021/acsomega.1c00310
33. Bauer, A.W., W.M.M. Kirby, J.C. Sherris and M. Turck, 1966. Antibiotic susceptibility testing by standardized disk method. *Am. J. Clin. Pathol.*, 45(4): 493–496. https://doi.org/10.1093/ajcp/45.4_ts.493
34. Bekele, S.G., D.D. Ganta and M. Endashaw, 2024. Green synthesis of ZnO nanoparticles using *Monoon longifolium*. *Discover Chem.*, 1(1). https://doi.org/10.1007/s44371-024-00007-9
35. Kumie, B., W. Wubet, T. Bizuayehu, H. Tegenu, M. Ababay and A. Melese, 2025. Green synthesis and antibacterial investigation of ZnO nanoparticles. *S. Afr. J. Chem. Eng.* https://doi.org/10.1016/j.sajce.2025.08.007
36. Brand-Williams, W., M.E. Cuvelier and C. Berset, 1995. Use of free radical method to evaluate antioxidant activity. *LWT-Food Sci. Technol.*, 28(1): 25–30. https://doi.org/10.1016/S0023-6438(95)80008-5
37. Adamu, T.B., A.M. Mengesha, M.A. Kebede, B.L. Bogale and T.W. Kassa, 2024. Biosynthesis of ZnO nanoparticles using *Lupinus albus*. *Results Chem.*, 10: 101724. https://doi.org/10.1016/j.rechem.2024.101724
38. Bizuayehu, T., B. Kassaw and M. Kendie, 2025. Green synthesis of ZnO nanoparticles using *Rumex nervosus*. *Results Chem.*, 102046. https://doi.org/10.1016/j.rechem.2025.102046
39. Azad, A., H. Zafar, F. Raza and M. Sulaiman, 2023. Factors influencing green synthesis of metallic nanoparticles. *Pharm. Front.*, 5(3): e117–e131. https://doi.org/10.1055/s-0043-1774289
40. Melkamu, W.W. and L.T. Bitew, 2021. Green synthesis of silver nanoparticles using *Hagenia abyssinica*. *Heliyon*, 7(11): e08459. https://doi.org/10.1016/j.heliyon.2021.e08459
41. Miu, B.A. and A. Dinischiotu, 2022. New green approaches in nanoparticle synthesis. *Molecules*, 27(19): 6472. https://doi.org/10.3390/molecules27196472
42. Xu, J., Y. Huang, S. Zhu, N. Abbes, X. Jing and L. Zhang, 2021. Green synthesis of ZnO nanoparticles for antibacterial textiles. *J. Eng. Fibers Fabr.*, 16. https://doi.org/10.1177/15589250211046242
43. Zeghoud, S., H. Hemmami, B.B. Seghir, I.B. Amor, I. Kouadri, A. Rebiai, M. Messaoudi, S. Ahmed, P. Pohl and J. Simal-Gandara, 2022. Biogenic synthesis of ZnO nanoparticles. *Mater. Today Commun.*, 33: 104747. https://doi.org/10.1016/j.mtcomm.2022.104747
44. Jafarirad, S., M. Mehrabi, B. Divband and M. Kosari-Nasab, 2015. Biofabrication of ZnO nanoparticles using *Rosa canina*. *Mater. Sci. Eng. C*, 59: 296–302. https://doi.org/10.1016/j.msec.2015.09.089
45. Awwad, A.M., B. Albiss and A.L. Ahmad, 2014. Green synthesis of ZnO nanosheets using *Olea europaea*. *Adv. Mater. Lett.*, 5(9): 520–524. https://doi.org/10.5185/amlett.2014.5575
46. El-Belely, E.F., M.M.S. Farag, H.A. Said, A.S. Amin, E. Azab, A.A. Gobouri and A. Fouda, 2021. Green synthesis of ZnO nanoparticles using *Arthrospira platensis*. *Nanomaterials*, 11(1): 95. https://doi.org/10.3390/nano11010095
47. Gajendran, P. and S. Kannappan, 2021. *Leonotis nepetifolia* mediated synthesis of ZnO nanoparticles. *SSRN Electron. J.* https://doi.org/10.2139/ssrn.3886321
48. Yuvakkumar, R., J. Suresh, B. Saravanakumar, A.J. Nathanael, S.I. Hong and V. Rajendran, 2014. Rambutan peel-mediated synthesis of ZnO nanochains. *Spectrochim. Acta A*, 137: 250–258. https://doi.org/10.1016/j.saa.2014.08.022
49. Alamdari, S., M.S. Ghamsari, C. Lee, W. Han, H. Park, M.J. Tafreshi, H. Afarideh and M.H.M. Ara, 2020. Preparation of ZnO nanoparticles using *Sambucus ebulus*. *Appl. Sci.*, 10(10): 3620. https://doi.org/10.3390/app10103620
50. Balogun, S.W., O.O. James, Y.K. Sanusi and O.H. Olayinka, 2020. Green synthesis of ZnO nanoparticles using *Mimosa pudica*. *SN Appl. Sci.*, 2(3). https://doi.org/10.1007/s42452-020-2127-3
51. Irfan, N.S.M. and N.K.H. Bhatti, 2023. ZnO nanoparticles mitigate cadmium toxicity in *Capsicum annuum*. *Proc. Pak. Acad. Sci. B*, 60(3). https://doi.org/10.53560/ppasb(60-3)854
52. Abdelmigid, H.M., N.A. Hussien, A.A. Alyamani, M.M. Morsi, N.M. AlSufyani and H.A. Kadi, 2022. Green synthesis of ZnO nanoparticles using pomegranate peel and coffee grounds. *Molecules*, 27(4): 1236. https://doi.org/10.3390/molecules27041236
53. Venkateasan, A., R. Prabakaran and V. Sujatha, 2017. Phytoextract-mediated synthesis of ZnO nanoparticles using *Ipomoea pes-*

caprae. *Nanotechnol. Environ. Eng.*, 2(1). https://doi.org/10.1007/s41204-017-0018-7
54. Barzinjy, A.A. and H.H. Azeez, 2020. Green synthesis of ZnO nanoparticles using *Eucalyptus globulus*. *SN Appl. Sci.*, 2(5). https://doi.org/10.1007/s42452-020-2813-1
55. Khoshhesab, Z.M., M. Sarfaraz and M.A. Asadabad, 2011. Preparation of ZnO nanostructures by chemical precipitation. *Synth. React. Inorg. Met.-Org. Nano-Met. Chem.*, 41(7): 814–819. https://doi.org/10.1080/15533174.2011.591308
56. Elumalai, K. and S. Velmurugan, 2015. Green synthesis of ZnO nanoparticles using *Azadirachta indica*. *Appl. Surf. Sci.*, 345: 329–336. https://doi.org/10.1016/j.apsusc.2015.03.176
57. Farooq, A., U.A. Khan, H. Ali, M. Sathish, S.A.H. Naqvi, S. Iqbal, I. Mubeen, M.B. Amir and W.F.A. Mosa, 2022. Green synthesis of ZnO nanoparticles using *Calotropis gigantea*. *Microorganisms*, 10: 2195. https://doi.org/10.3390/microorganisms10112195
58. Mohammadi, C., S. Mahmud, S.M. Abdullah and Y. Mirzaei, 2017. Green synthesis of ZnO nanoparticles using *Euphorbia petiolata*. *Morocc. J. Chem.*, 5(3). https://doi.org/10.48317/imist.prsm/morjchem-v5i3.8974
59. Martínez, G., 2021. Erratum: Environmental impact of nanoparticles application. *Materials*, 14(7): 1–26. https://doi.org/10.3390/ma14071710
60. Raji, R. and K.G. Gopchandran, 2017. ZnO nanostructures with tunable luminescence. *J. Sci. Adv. Mater. Dev.*, 2(1): 51–58. https://doi.org/10.1016/j.jsamd.2017.02.002
61. Boukhris, M., M.S.J. Simmonds, S. Sayadi and M. Bouaziz, 2012. Chemical composition and biological activities of *Pelargonium graveolens*. *Phytother. Res.*, 27(8): 1206–1213. https://doi.org/10.1002/ptr.4853
62. Weng, X., M. Guo, F. Luo and Z. Chen, 2016. One-step green synthesis of Fe/Ni nanoparticles. *Chem. Eng. J.*, 308: 904–911. https://doi.org/10.1016/j.cej.2016.09.134
63. Mittal, A.K., Y. Chisti and U.C. Banerjee, 2013. Synthesis of metallic nanoparticles using plant extracts. *Biotechnol. Adv.*, 31(2): 346–356. https://doi.org/10.1016/j.biotechadv.2013.01.003
64. Sathiyavimal, S., S. Vasantharaj, D. Bharathi, M. Saravanan, E. Manikandan, S.S. Kumar and A. Pugazhendhi, 2018. Biogenesis of CuO nanoparticles using *Sida acuta*. *J. Photochem. Photobiol. B*, 188: 126–134. https://doi.org/10.1016/j.jphotobiol.2018.09.014
65. Bharathi, D., S. Vasantharaj and V. Bhuvaneshwari, 2018. Green synthesis of silver nanoparticles using *Cordia dichotoma*. *Mater. Res. Express*, 5(5): 055404. https://doi.org/10.1088/2053-1591/aac2ef
66. Basak, G., D. Das and N. Das, 2014. Dual role of sophorolipid in ZnO nanoparticle synthesis. *J. Microbiol. Biotechnol.*, 24(1): 87–96. https://doi.org/10.4014/jmb.1307.07081
67. Fatimah, I., R.Y. Pradita and A. Nurfalinda, 2016. Plant extract-mediated synthesis of ZnO nanoparticles. *Procedia Eng.*, 148: 43–48. https://doi.org/10.1016/j.proeng.2016.06.483
68. Bindhu and M. Umadevi, 2014. Antibacterial activities of green synthesized gold nanoparticles. *Mater. Lett.*, 120: 122–125. https://doi.org/10.1016/j.matlet.2014.01.108
69. Muthukumar, T., N. Sudhakumari, B. Sambandam, A. Aravinthan, T.P. Sastry and J. Kim, 2016. Green synthesis of gold nanoparticles. *Process Biochem.*, 51(3): 384–391. https://doi.org/10.1016/j.procbio.2015.12.017
70. Allen, H.K., J. Donato, H.H. Wang, K.A. Cloud-Hansen, J. Davies and J. Handelsman, 2010. Antibiotic resistance genes in natural environments. *Nat. Rev. Microbiol.*, 8(4): 251–259. https://doi.org/10.1038/nrmicro2312
71. Romaniuk, J.A.H. and L. Cegelski, 2015. Bacterial cell wall composition and antibiotic influence. *Phil. Trans. R. Soc. B*, 370(1679): 20150024. https://doi.org/10.1098/rstb.2015.0024
72. Heesterbeek, D.A.C., N.I. Martin, A. van Velthuizen, M. Duijst, M. Ruyken, R. Wubbolts, S.H.M. Rooijakkers and B.W. Bardoel, 2019. Complement-dependent membrane perturbation. *Sci. Rep.*, 9(1). https://doi.org/10.1038/s41598-019-43208-4
73. Davies, J. and D. Davies, 2010. Origins and evolution of antibiotic resistance. *Microbiol. Mol. Biol. Rev.*, 74(3): 417–433. https://doi.org/10.1128/mmbr.00016-10
74. Bamigboye, M., 2025. Green synthesis of ZnO nanoparticles using *Microtrichia perotitii*. *Aswan Univ. J. Sci. Technol.*, 5(1): 1–11. https://doi.org/10.21608/aujst.2024.308279.1114
75. Belay, A., C.R. Ar and B.Z. Z, 2017. Synthesis and characterization of ZnO nanoparticles. *J. Nanomed. Nanotechnol.*, S8. https://doi.org/10.4172/2157-7439.s8-004
76. Gunalan, S., R. Sivaraj and V. Rajendran, 2012. Green synthesized ZnO nanoparticles against pathogens. *Prog. Nat. Sci. Mater. Int.*, 22(6): 693–700. https://doi.org/10.1016/j.pnsc.2012.11.015
77. Yang, Z. and C. Xie, 2006. Zn^{2+} release from zinc and ZnO particles. *Colloids Surf. B*, 47(2): 140–145. https://doi.org/10.1016/j.colsurfb.2005.12.007
78. Soren, S., S. Kumar, S. Mishra, P.K. Jena, S.K. Verma and P. Parhi, 2018. Antibacterial and antioxidant potential of ZnO nanoparticles. *Microb. Pathog.*, 119: 145–151. https://doi.org/10.1016/j.micpath.2018.03.048
79. Nair, S., A. Sasidharan, V.V.D. Rani, D. Menon, K. Manzoor and S. Raina, 2008. Size-dependent toxicity of ZnO particles. *J. Mater. Sci. Mater. Med.*, 20(S1): 235–241. https://doi.org/10.1007/s10856-008-3548-5
80. Agarwal, N.H., N.S. Menon, S.V. Kumar and S. Rajeshkumar, 2018. Mechanistic study on antibacterial action of ZnO nanoparticles. *Chem.-Biol. Interact.*, 286: 60–70. https://doi.org/10.1016/j.cbi.2018.03.008
81. Jayaseelan, C., A.A. Rahuman, A.V. Kirthi, S. Marimuthu, T. Santhoshkumar, A. Bagavan, K. Gaurav, L. Karthik and K.B. Rao, 2012. Microbial synthesis of ZnO nanoparticles using *Aeromonas hydrophila*. *Spectrochim. Acta A*, 90: 78–84. https://doi.org/10.1016/j.saa.2012.01.006
82. Abomuti, M.A., E.Y. Danish, A. Firoz, N. Hasan and M.A. Malik, 2021. Green synthesis of ZnO nanoparticles using *Salvia officinalis*. *Biology*, 10(11): 1075. https://doi.org/10.3390/biology10111075
83. Tan, E.P., S. Djearamane, L.S. Wong, R. Rajamani, A.C.T. Antony, S.K. Subbaih, A.K. Janakiraman, M. Aminuzzaman, V. Subramaniyan, M. Sekar and S. Selvaraj, 2022. Antifungal efficacy of ZnO nanoparticles against *Saccharomyces cerevisiae*. *Coatings*, 12(12): 1988. https://doi.org/10.3390/coatings12121988